

Reduction and Oxidation Doping Kinetics of an Electropolymerized Donor–Acceptor Low-Bandgap Conjugated Copolymer

J. Arias-Pardilla,[†] W. Walker,[‡] F. Wudl,[‡] and T. F. Otero^{*,†}

Group of Electrochemistry, Intelligent Materials and Devices (GEMDI), Universidad Politécnica de Cartagena, ETSII, E- 30203, Cartagena, Spain, and Center for Polymers and Organic Solids, University of California, Santa Barbara, California 93106

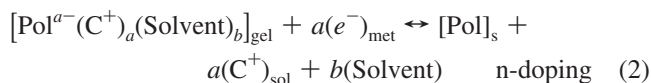
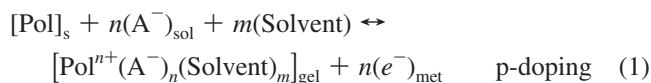
Received: April 29, 2010; Revised Manuscript Received: August 23, 2010

The electrochemical synthesis of a new dithienylcyclopentadienone-derivative/3-methylthiophene copolymer was performed by cyclic voltammetry. The obtained material shows redox processes very close to those from the pristine DTCPD. A new redox process at -1.24 V, with a large anodic shift (0.51 V) related to the poly(3-methylthiophene) reduction, indicates the existence of a copolymer with a strong influence of the neighboring (n-doped) DTCPD comonomer. The new copolymer is electrochemically n-doped at more cathodic potentials than -750 mV and p-doped at more anodic potentials than 250 mV, with a bandgap of 1.0 eV. The cation's entrance in the film from the solution during n-doping and anion's entrance during p-doping for charge balance was checked by QCM. The reduction of the DTCPD part suffers a partial trapping of the negative charges that can be reoxidized only at high overpotentials (>1 V related to the reduction potentials). After polarization of the material at any potential inside the band gap, subsequent p- or n-doping reactions performed by potential steps start by nucleation–relaxation kinetic control, followed by anodic or cathodic, respectively, chronoamperometric maxima. At the maxima, both reactions were checked to occur under chemical kinetic control, allowing the determination of the reaction orders for p- and n-doping processes.

Introduction

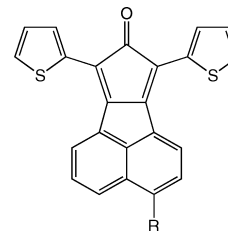
Organic conjugated materials have been studied very intensively as active materials for different applications as supercapacitors,^{1,2} batteries^{3,4} or low-cost organic thin-film transistors (OTFT).^{5,6} Recently, properties from a family of compounds derived from dithienylcyclopentadienone have attracted much attention, revealing a broad absorption band covering practically the whole visible region⁷ and having an atypical correlation between absorption and photoresponse.⁸

Those materials are conjugated conducting polymers that are both p- and n-dopable, such as PEDOT,^{9,10} polythiophene,^{11,12} or polyfluorenes.^{13,14} These polymers are able to store positive and negative charges along the backbone during oxidation or reduction reactions with simultaneous insertion of charge-compensating counterions through the following general simplified reactions,



where Pol^+ and Pol^- represent the active sites in the polymer able to store positive or negative charges; C^+ and A^- are the cations or anions of the electrolyte; Solvent is solvent molecules required for osmotic pressure balance inside the polymer; and

SCHEME 1: Structure of 2-Ethylheptyl-DTCPD



2-ethylheptyl-DTCPD

R = 2-ethylheptyl

the subscripts s, sol, gel, and met are solid, solution, gel, and metal states, respectively.

Reaction kinetics of the p-doping processes have been widely studied from chronoamperometric results for different conducting polymers, such as polypyrrole,^{15,16} polyaniline,^{17,18} polythiophenes,^{19,20} or PEDOT,²¹ in accord with the electrochemically stimulated conformational relaxation (ESCR) model.^{22,23} In contrast, n-doping processes have received rather limited attention from a kinetic point of view. The high negative potentials usually required for n-doping promote reactions with residual water and oxygen, causing partial degradation, which makes kinetic studies quite difficult.

In this article, we report the electrochemical copolymerization of 2-ethylheptyl-DTCPD (Scheme 1) with 3-methylthiophene. The electrochemical copolymerization is an interesting way to include a monomer having a low reactivity, or nonreactive, in a polymer chain. A DTCPD copolymer was previously obtained by a chemical process.⁸ Here, we try to obtain polymer films by electropolymerization, choosing as comonomer 3-methylthiophene, looking for some compatibility with the thiophene rings

* Corresponding author. E-mail: toribio.fotero@uptc.es.

[†] Universidad Politécnica de Cartagena.

[‡] University of California, Santa Barbara.

present in DTCPD. We have electrochemically characterized the oxidation–reduction processes in the copolymer film, and finally, we have investigated the oxidation kinetics of both p- and n-doping, trying to check if the ESCR model is also valid for n-doping.

Experimental Section

Dichloromethane (Fluka) and acetonitrile (Sigma Aldrich) were used after drying using a molecular sieve UOP Type 3A (Fluka). Tetrabutylammonium hexafluorophosphate (Fluka) (TBAPF_6) was used as received. 3-Methylthiophene (Sigma Aldrich) was purified by distillation under vacuum using a diaphragm vacuum pump MZ 2C (Schott) and stored under nitrogen atmosphere at -10°C . See references 7 and 8 as well as the Supporting Information for the synthesis details of 2-ethylheptyl-DTCPD.

All electrochemical studies were performed using an Autolab PGSTAT-100 potentiostat/galvanostat controlled by a personal computer using the GEPES electrochemical software, in a three-electrode cell, under a nitrogen atmosphere at ambient temperature. A platinum sheet of 1 cm^2 surface area was used as the working electrode, and two stainless steel sheets having 4 cm^2 of surface were used as the counterelectrode during electropolymerization. Ag/AgCl (3 M KCl) supplied by Metrohm was the reference electrode.

For the electrochemical quartz microbalance measurements, an EG&G PAR model QCA917 microbalance was used. The electrodes used were AT-cut 9 MHz piezoelectric crystals, coated with Pt ($0.3\text{ }\mu\text{m}$ thick) deposited over a Ti adhesion layer (50 nm thick), with an area of 0.196 cm^2 . A capacitance of 1 nF was used to isolate the potentiostat from the microbalance. The linearity of the relation between resonant frequency and the change in crystal mass was verified by platinum and silver deposition and the Sauerbrey equation. This equation was used to calculate mass changes from frequency changes with an integral sensitivity of $1.8 \times 10^8\text{ Hz cm}^{-2}\text{ g}^{-1}$.

The electrochemical oxidation and copolymerization were studied by cyclic voltammetry (CV) in 0.001 M 2-ethylheptyl-DTCPD + 0.005 M 3-methylthiophene solutions in dichloromethane and 0.1 M TBAPF_6 as electrolyte. Dichloromethane was used due to the high solubility of both monomers and electrolyte in this solvent.

The electrochemical control of the generated films and the ionic interchanges were conducted in 0.1 M TBAPF_6 acetonitrile solution.

Results and Discussion

Electrochemical Characterization of 2-Ethylheptyl-DTCPD Monomer. The electrochemical behavior of the novel DTCPD derivative was investigated by cyclic voltammetry in dichloromethane. In Figure 1 are depicted voltammetric responses from a clean platinum electrode performed at 50 mV s^{-1} , between -1.60 V and different anodic potentials. The dotted line shows the voltammogram corresponding to the background electrolyte: 0.1 M TBAPF_6 in dichloromethane. The solid line voltammograms were obtained from 1 mM 2-ethylheptyl-DTCPD plus a 0.1 M TBAPF_6 dichloromethane solution. On the anodic sweep, four oxidation processes are present at -1.27 , -0.70 , 1.03 , and 1.70 V before the beginning of the background electrolyte oxidation at $\sim 2.00\text{ V}$ (dotted line). On the negative sweep, two different reduction processes can be observed at -0.85 and -1.44 V before the reduction of the background electrolyte starts at around -1.6 V . These reduction processes are related to the oxidations observed at -1.27 and -0.70 V ,

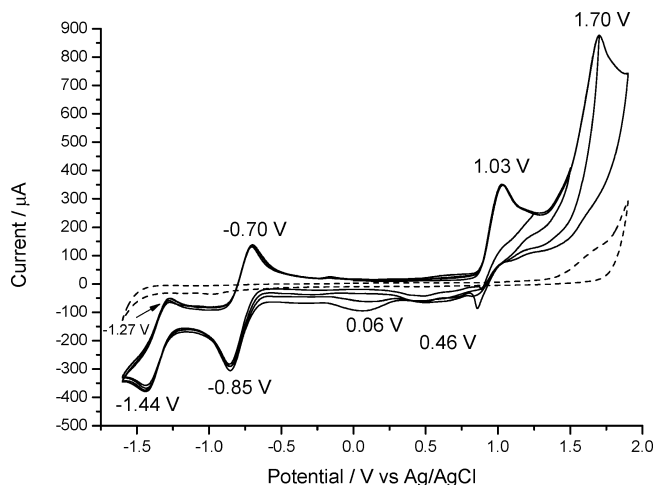


Figure 1. Cyclic voltammograms obtained in 1 mM 2-ethylheptyl-DTCPD and 0.1 M TBAPF_6 dichloromethane solution for different anodic potential limits (—) and in the absence of monomer (····) using a 1 cm^2 Pt electrode. Initial potential, -1.60 V ; scan rate, 50 mV s^{-1} ; temperature, 20°C .

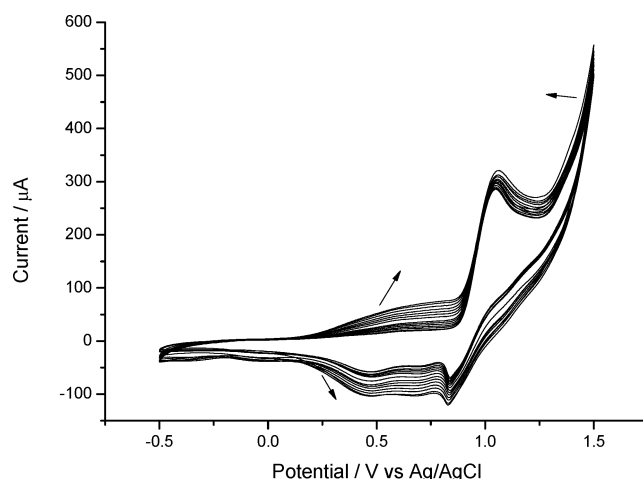


Figure 2. Consecutive cyclic voltammograms obtained in 1 mM 2-ethylheptyl-DTCPD + 5 mM 3-methylthiophene and 0.1 M TBAPF_6 dichloromethane solution using a 1 cm^2 (0.5 cm^2 sheet) Pt electrode, sweeping the potential from -0.50 to 1.50 V . Scan rate, 50 mV s^{-1} ; temperature, 20°C .

forming two redox couples with $E^0 = -1.36$ and -0.81 V , similar to those previously observed in other compounds of the same chemical family.^{7,8} The narrow and electrochemical reversible nature of the reduction waves reflects the highly localized state of the radical anion and dianion on the cyclopentadiene moiety.^{7,8} The oxidation processes at 1.03 and 1.70 V present a higher irreversibility. Consecutive potential sweeps applied up to anodic potential limits including those maxima do not produce any deposit on the electrode surface, pointing to a high solubility of the oxidized products.

Electrochemical Copolymerization of 2-Ethylheptyl-DTCPD with 3-Methylthiophene. From a solution including two monomers, 5 mM 3-methylthiophene and 1 mM 2-ethylheptyl-DTCPD in the same electrolyte, the consecutive voltammograms shown by Figure 2 were obtained by cycling the potential between -0.5 and 1.5 V . A fast increase in the current is observed at potentials more anodic than 1.25 V . A new broad oxidation–reduction process appears between 0.30 and 0.85 V that increases on the consecutive voltammograms, indicating the presence of an increasing amount of electroactive material electrogenerated during every anodic sweep over 1.20 V . This

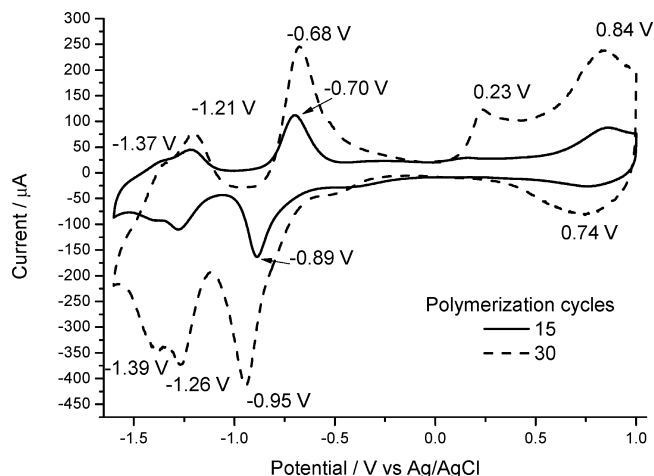


Figure 3. Stabilized voltammograms obtained from poly(2-ethylheptyl-DTCPD-co-3-methylthiophene) films, using as cycling potential limits -1.60 and 1.00 V and 50 mV s^{-1} as the potential scan rate. The two films were electrogenerated in fresh monomeric solutions after 15 (—) or 30 (---) consecutive cycles, as indicated in Figure 2.

is the expected voltammetric response for the electrogeneration of electroactive materials.

Electrochemical Control of the Electrogenerated Material.

Two films of the electrogenerated polymer were obtained by applying 15 or 30 consecutive potential cycles to a clean Pt electrode under the same conditions and using a fresh solution every time. Each coated electrode was transferred, after rinsing with the solvent, into 0.1 M TBAPF₆ acetonitrile solution. Figure 3 shows the result of the voltammetric characterizations by cycling between -1.60 and 1.00 V.

The thinner film exhibits four redox processes. The oxidation–reduction maxima at 0.84 and 0.74 V, respectively (standard potential $E^0 = 0.79$ V) overlaps the oxidation/reduction potentials of the parent poly(3-methylthiophene) polymer.²⁴ That should mean the extraction of electrons from the polymer during the oxidation sweep, with generation of positive charges (p-doping) and entrance of balancing anions from the solution. The processes should be reversed during the reduction sweep.

Two of the other three redox processes, with standard potentials at -0.80 and -1.38 V, are close to similar ones described above for 2-ethylheptyl-DTCPD, indicating its presence in the film. That should mean the injection of electrons during the reduction sweep with generation of negative charges on the chains (n-doping) and entrance of balancing cations from the solution. The redox process present at $E^0 = -1.38$ V is close to that observed for the 2-ethylheptyl-DTCPD at -1.36 V, showing now a greater reversibility (smaller potential difference between oxidation and reduction peaks), pointing to the inclusion of the molecule in the polymer chain. The new redox process, related to those of the 2-ethylheptyl-DTCPD, at -1.24 V could indicate the participation of the 3-methylthiophene fraction. A similar film of poly(3-methylthiophene), generated under the same monomer concentration and oxidation potential, can be irreversibly reduced only at -1.75 V (Supporting Information). This large shift indicates a strong influence of the neighboring n-doped comonomer, supporting the generation of a copolymer during the electropolymerization.

The thicker film generated by 30 polymerization cycles presents the same 4 redox processes. Now the process at -0.81 V shows a greater separation between oxidation (-0.68 V) and reduction (-0.95 V) peaks, indicating a higher irreversibility of the process related to the rising resistance of the thicker film

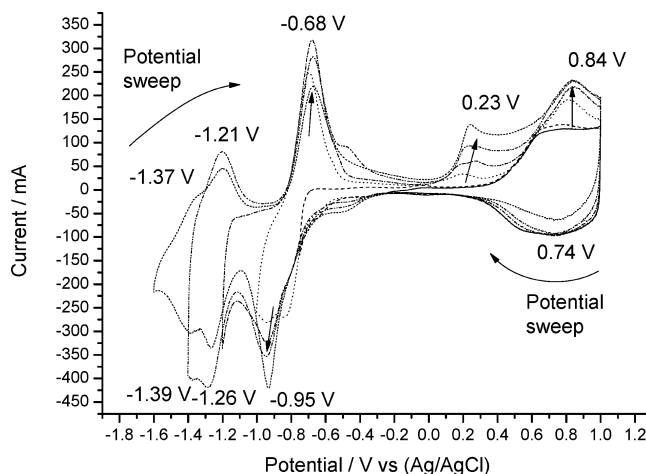


Figure 4. Voltammograms obtained from a poly(2-ethylheptyl-DTCPD-co-3-methylthiophene) film in 0.1 M TBAPF₆ acetonitrile solution at 50 mV s^{-1} and 20 °C for different cathodic potential limits: (—) -0.25 V, (---) -0.75 V, (·····) -1.00 V, (— · — · —) -1.25 V, (— · — · — · —) -1.40 V and (— · — · — · — · —) -1.60 V.

for the penetration/expulsion of balancing counterions. In general, an increase in the voltammetric charges (related to those of the thinner film) is observed for the different processes. Moreover, a clear irreversible oxidation process is present at 0.23 V without any corresponding reduction.

Trapping Charge. Trying to clarify the origin of this new oxidation process, we submitted the material to consecutive voltammograms, starting every time from the oxidized material at the anodic potential of 1.00 V and reducing it by cathodic potential sweeps up to different (increasing) cathodic potential limits (Figure 4). The oxidation charge involved in the new oxidation process starts at a cathodic potential limit of -0.75 V and increases for rising cathodic potential limits. The latter behavior suggests that this oxidation process involves charge trapping, as previously observed in PEDOT^{25,26} or polypyrrole²⁷-functionalized films. A fraction of the negative charges stored in the chains by reduction between -0.75 and -1.5 V remain trapped, being reoxidized only at potentials more anodic than -0.10 V, overlapping the oxidation processes that store positive charges on the chains.

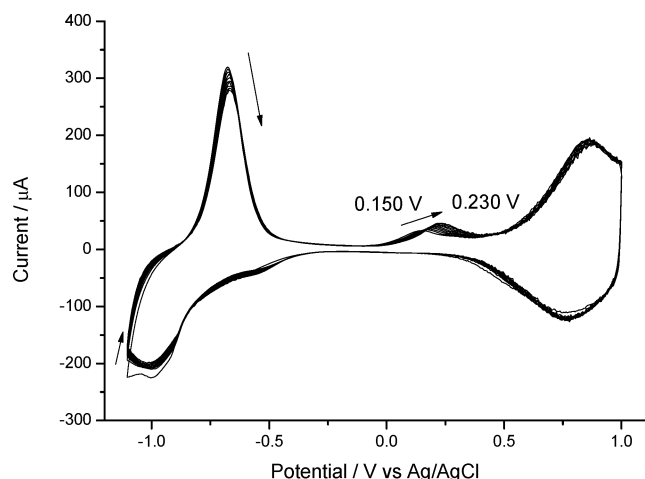
The percentage of trapped charge was calculated by integration of the anodic voltammograms between -0.25 and 1.00 V (Q_1) minus the charge on the same potential range in the absence of the trapping effect (Q_2), divided by the full oxidation charge of the voltammogram (the Q_3), minus Q_2 . This percentage attains 66% for a cathodic limit inside the first n-doping voltammetric maximum and rises from 31 to 51% when the cathodic potential limit moves from -1.00 to -1.60 V in the potential range of the second n-doping process (Table 1 and Supporting Information). This trapping effect has been attributed to the insulating or low-conductivity state of the polymer matrix and the charge transfer by a hopping mechanism between DTCPPD units at cathodic potentials.²⁸

In our material, the low potential difference between the three anodic and cathodic maxima for the most reversible fraction of the processes at 50 mV s^{-1} should indicate a high enough conductivity and a different chemical or structural origin for the n-doped fraction that requires such a high anodic overpotential to be reoxidized to the neutral state. The trapped percentage at -0.75 V is related to a very low total charge. Coming into the regions of the most important charges, the trapping percentage increases with the cathodic potential limit

TABLE 1: Charges Obtained by Integration between Different Potential Limits of the Voltammetric Responses from Figure 4, Obtained for Different Cathodic Potential Limits^a

cathodic potential limit (V)	total anodic charge (C) (Q_3)	Q_1 (C)	trapped charge (C) $Q_1 - Q_2$	trapped %
-0.25	1.296×10^{-3} (Q_2)			
-0.75	1.42×10^{-3}	1.38×10^{-3}	8.40×10^{-5}	66
-1.00	2.63×10^{-3}	1.73×10^{-3}	4.37×10^{-4}	33
-1.20	3.30×10^{-3}	2.07×10^{-3}	7.72×10^{-4}	38
-1.40	4.01×10^{-3}	2.42×10^{-3}	1.12×10^{-3}	41
-1.60	4.18×10^{-3}	2.73×10^{-3}	1.43×10^{-3}	49

^a Q_1 , the oxidation charge between -0.25 and 1.00 V; Q_2 , the oxidation charge consumed by p-doping between -0.25 and 1.00 V obtained from the voltammogram performed inside the same potential limits; Q_3 , the full oxidation charge involved in each voltammogram. The trapping charge percentage is giving by $100 \times (Q_1 - Q_2)/(Q_3 - Q_2)$.

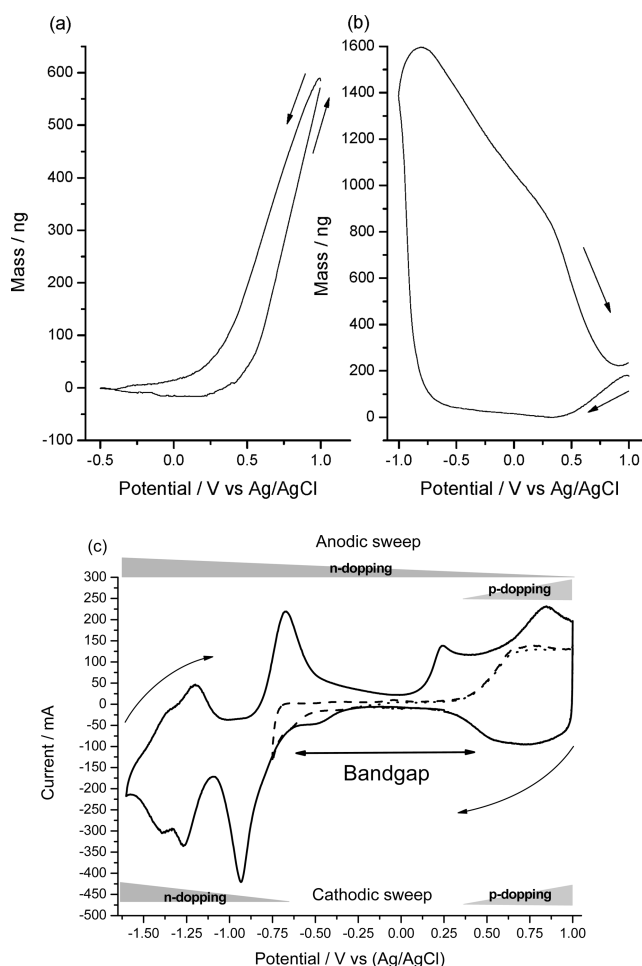
**Figure 5.** Ten consecutive voltammograms obtained after experiments from Figure 4, under similar conditions, between 1.00 and -1.10 V.

from -0.75 to -1.60 V, indicating a strong polymer-cation interaction when the polymer moves from anion radical states, around the potential maximum at -0.95 V, these linked to the more cathodic maxima.

A remarkable fact: the total charge stored by n-doping is 2.6 times greater than the charge stored by p-doping, opening great expectations for batteries or supercapacitors applications.

After these experiments, a new potential sweep between 1.00 and -0.50 V overlaps the initial response (Figure 4, solid line) pointing to a good stability of the film under cycling. The material's stability was studied by cycling between 1.00 and -1.10 V for 10 consecutive cycles. A slow decline in both anodic and cathodic charges (Figure 5) of ~5% was observed. This value is much lower than that observed in other materials under similar experimental conditions.²⁶ The percentage of trapped charge remains constant on every cycle.

Mass Variations. To try to corroborate the ionic interchanges, films were electrogenerated on quartz crystal microbalance electrodes and then studied by cyclic voltammetry. Figure 6 shows the results. The potential cycle was started from oxidized state of the material at 1.00 V going up to -0.50 V and back to the initial potential to work in the absence of trapping effects. The mass of the film decreases, Figure 6a, by electrochemical reduction and is recovered by oxidation back to 1.00 V. The main interchange of mass occurs between 0.25 and 1.00 V. This variation suggests the entrance, or expulsion, of balancing anions during oxidation or reduction, respectively required to compensate the positive charges generated/eliminated along the polymer chains. Apparent molar masses of 316 g mol^{-1} during p-dedoping and 343 g mol^{-1} for doping processes were obtained. They are larger than the 145 g mol^{-1} PF_6^- anion, requiring the interchange of at least four solvent molecules in parallel to the

**Figure 6.** Mass changes obtained from a film electrogenerated on quartz crystal microbalance electrode during potential cycling in the background electrolyte at 50 mV s^{-1} (a) between 1.00 and -0.50 V or (b) between 1.00 and -1.00 V. The potential sweep always was initiated from the oxidized state at 1.00 V. (c) Evolution of p- and n-doping processes along the anodic and cathodic potential sweeps, in accordance with voltammetric and mass variation results. Dotted voltammogram shows the p-doping/dedoping domain. Dashed voltammogram indicates the beginning of the n-doping process, allowing the determination of the bandgap. Full line voltammogram shows all the p and n doping/dedoping processes.

anion's interchange. Differences between apparent masses during the doping/dedoping processes should confirm the movement of solvent molecules. In any case, the apparent masses are higher than that previously obtained with the same electrolyte and solvent for a bithiophene derivative.²⁹ The interchange of anions is very fast, and the hysteresis between oxidation and reduction mass evolutions is quite small (see below for cations interchange). Those results suggest the presence of fast swelling processes during anion's entrance.

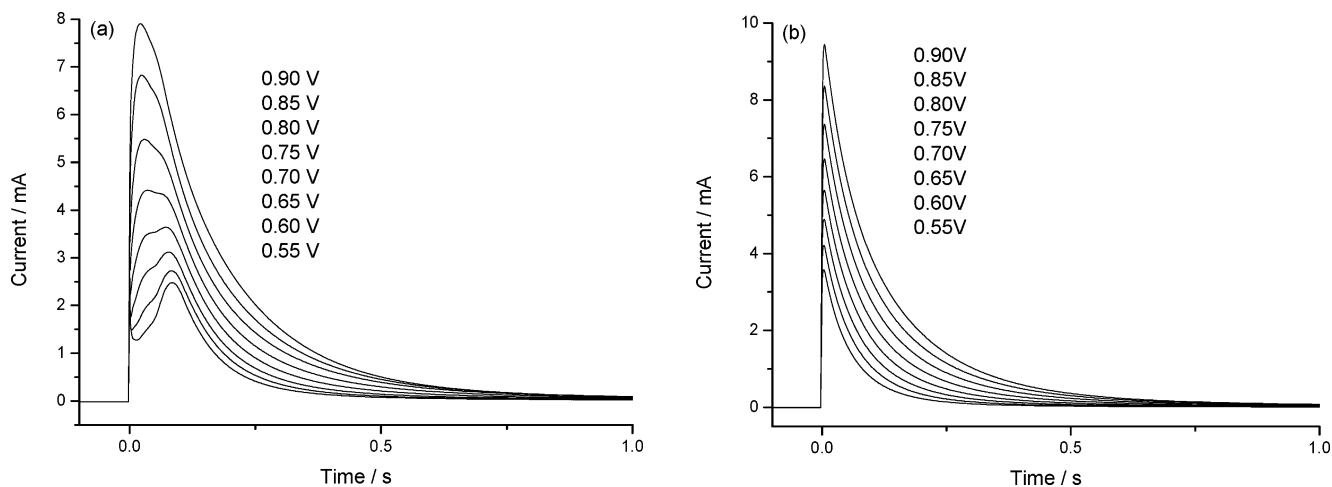


Figure 7. Chronoamperometric responses of a poly(2-ethylheptyl-DTCPD-co-3-methylthiophene)-coated platinum electrode in 0.1 M TBAPF₆ acetonitrile solution, submitted to potential steps from (a) -0.50 and (b) 0.10 V cathodic potentials maintained for 10 s to different anodic potentials indicated in the figure.

Starting from the same initial potential (1.00 V) by potential sweep up to the cathodic potential limit of -1.00 V, the mass decreases (Figure 6b) by anion expulsion until 0.25 V. At -0.75 V, a fast increase in the mass is observed that can be correlated to the insertion of cations, required to balance negative charges injected on chains. The mass increase goes on even at the beginning of the following anodic sweep, pointing to a slow entrance of cations during the cathodic sweep far away from the equilibrium conditions. The average apparent mass in this potential range is 309 g mol^{-1} , again exceeding 242.5 g mol^{-1} , corresponding to TBA⁺. The cation should move together solvent molecules in a 2:3 ratio. This apparent molar mass is closed to 330 g mol^{-1} previously obtained with bithiophene derivatives under similar conditions.²⁹

These results suggest a packed structure of the chain conformations for the n-doped material with a low interchange of the studied solvent and low swelling ratio (low volume fraction change per unit of charge). At potentials more anodic than -0.50 V, the mass starts to decrease. These expulsions of balancing cations are far from complete before the anions start their entry at potentials more anodic than 0.25 V. The beginning of this entrance stimulates a fast increase in the expulsion rate. This expulsion rate is so high that the overall mass variation decreases faster between 0.25 and 1.00 V, where the cation expulsion now overlaps the entrance of anions, than when only the expulsion of cations was present between -0.5 and 0.25 V. At the end of the cycle, a small increase in the material mass is observed, related to that of the beginning. Those overlapping processes give an apparent molar mass changing from 310 to 155 g mol^{-1} , requiring deeper study to obtain some quantitative explanation.

Potential Ranges of p- and n-Doping Processes. Voltammetric and CQM results indicate that the most neutral state of the polymer film (very low density of charges on chains) is present between 0.40 and -0.75 V, and the material is expected to present a packed conformational structure. The low stored charge density will produce strong polymer–polymer, inter- and intramolecular, attractive interactions, tightening the structure. At potentials more anodic than 0.40 V, the material oxidizes: electrons are extracted from the material chains, generating positive charges (p-doping). Anions are forced to penetrate from the solution for charge balance, and the material swells. Starting again from the most neutral state, a cathodic potential sweep promotes the material reduction: electrons are injected to the

material chains, generating negative charges (n-doping) and requiring the penetration of cations from the solution for charge balance: the polymer film swells again, but now much more slowly than during p-doping. A good fraction of the charge stored during n-doping remains trapped up to high anodic overpotentials. The potential difference between starting p-doping and n-doping processes corresponds to a bandgap width of 1.0 eV.

The results mentioned above are collected in Figure 6c. Moreover, when the anodic potential sweep starts at potentials more cathodic than -0.75 V, the trapping effect is present, and the stored negative charges are compensated along the full anodic potential sweep. Over 31% of the full n-doping charge is compensated at the same time as the material is p-doped.

Under those conditions, starting from the material oxidized at 1.0 V, any subsequent reduction–polarization at a potential inside the -0.75 to 0.40 V potential range is expected to produce a compact structure of the most neutral material. Used as initial states, the ESCR model should predict that either the material oxidation or the material reduction should occur by penetration of anions or cations, respectively, through those points of the material/solution interface having a greater mobility (relaxation) of the chains, by nucleation–relaxation.^{22,23} Nucleation processes generate maxima on the chronoamperometric responses, so both the oxidation (p-doping) and the reduction (n-doping) processes studied by potential steps are expected to give chronoamperometric responses showing a maximum.

p-Doping Reaction Kinetics. The platinum electrode was coated after 30 cycles in 0.1 M TBAPF₆ dichloromethane solution. The oxidation (p-doping) process was studied by submitting the material to potential steps from -0.50 V, maintained for 10 s, to different anodic potentials ranging from 0.55 to 0.90 V (Figure 7a). The procedure was repeated starting now from 0.10 V and kept for 10 s (Figure 7b). The chronoamperograms show a well-defined peak, including two oxidation processes (a maximum and a shoulder). Oxidations at higher anodic potentials give rising currents at the maximum, the maximum shifts to shorter times, and the prevailing oxidation process (the one responsible for the higher current) changes; the shoulder appears at times shorter than the maximum for low oxidation potentials and becomes the maximum for high oxidation potentials. After reduction and packing at 0.10 V, only one well-defined oxidation maximum is observed at very short oxidation times. This maximum includes the two different

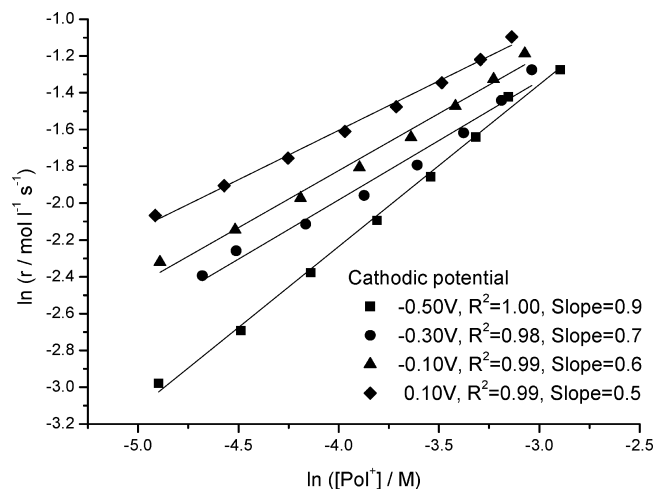


Figure 8. Double logarithmic plot of the oxidation rate of poly(2-ethylheptyl-DTCPD-*co*-3-methylthiophene) film submitted to potential steps between different indicated cathodic potentials, kept for 10 s every time, and different anodic potentials used in Figure 7 in 0.1 M TBAPF₆ acetonitrile solution.

processes observed after reduction at -0.50 V that now overlap when the initial state is attained by reduction at low reduction overpotential (0.10 V).

The chronoamperometric responses from Figure 8 represent the oxidation kinetics of the material. Considering the oxidation similar to reaction 1, the empirical kinetic equation for the oxidation rate, assuming a prevalent interchange of anions, should be

$$r(\text{mol L}^{-1} \text{s}^{-1}) = \frac{dQ}{FV dt} = k[\text{PF}_6^-]^\alpha [\text{Pol}^+]^\beta \quad (3)$$

This equation correlates the oxidation rate (r) with the anodic charge (Q) consumed during the oxidation reaction. α and β represent the reaction orders related to the concentration of counterions $[\text{PF}_6^-]$ in solution and to the concentration of active centers $[\text{Pol}^+]$ in the polymer film, respectively. k is the rate constant or rate coefficient. V is the volume of the polymer film and F is Faraday's constant. The active centers are those points of the polymer chains able to store a positive charge after oxidation. By integration of the chronoamperograms, we obtain the evolution of the oxidation rate as chronocoulograms (Q evolution as a function of t , see the Supporting Information). These are chemical kinetics showing an induction period. The initial oxidation rate, required for kinetic determinations, is the slope at the induction time (dQ/dt); this is the current at the original chronoamperometric maxima.

The concentration of active centers $[\text{Pol}^+]$ is obtained from the charge Q , consumed to oxidize the polymer film at the applied anodic potential, obtained by integration of the experimental chronoamperograms, the weight of the polymer film obtained by microgravimetry, and the material density (1.55 g cm^{-3})³⁰ as

$$[\text{Pol}^*] = \frac{Q}{FV} = \frac{Q\rho}{F \times \text{Mass}} \quad (4)$$

The way to check the validity of the kinetic expression (eq 3) is by changing one of the variables involved every time, keeping all the others constant. For instance, oxidation at different concentrations of active centers (potential step to

different anodic potentials) under constant temperature ($k = \text{constant}$) and constant electrolyte concentration. The oxidation starts from the same initial state of the material obtained by reduction at the same cathodic potential (inside the bandgap), applied for the same time.

By taking logarithms, the kinetic eq 3 becomes

$$\ln r = k' + \beta \ln[\text{Pol}^+] \quad (5)$$

Equation 5 allows checking if the reaction at the chronoamperometric maxima (the reaction rate, r , and the current, $i = dQ/dt$, are related through eq 3) occurs under chemical kinetic control.

Figure 8 shows the double logarithmic plot of the oxidation rates versus different concentrations of active centers. As expected from eq 5, a good fit of the experimental data is obtained, corroborating the chemical kinetic control of the p-doping process. Increasing slopes were obtained when the kinetics were studied from initial states obtained by reduction at rising cathodic potentials. The values of the reaction order β range between 0.5 and 0.9. As previously observed for the parent poly(3-methylthiophene)²⁴ and other different polymers and electrolyte-solvent systems,^{15,19} the oxidation of poly(2-ethylheptyl-DTCPD-*co*-3-methylthiophene) films using increasingly packed conformations of the polymeric structures as initial states promotes an increase in the reaction order related to the concentration of active centers in the polymer.

n-Doping Reaction Kinetics. The coated platinum electrode was then submitted to a similar methodology to check if the reduction maxima present on the voltammograms at potentials more cathodic than -0.50 V correspond to n-doping reactions, such as reaction 2, and if those reactions also are initiated from the neutral material through a nucleation process.

Figure 9a shows the chronoamperometric responses from the coated platinum electrode in 0.1 M TBAPF₆ acetonitrile solution when the material was submitted to potential steps from 0.25 V, maintained for 10s, to different cathodic potentials ranging from -1.00 to -1.30 V. The procedure was repeated, but recovering the neutral state of the material by oxidation at 0.00 V for 10 s (Figure 9b) before the potential step to the cathodic potentials. The responses related to the reaction from the neutral state to the reduced state show a reduction maximum, in a way similar to those oxidation maxima obtained for the transition from the neutral state to the oxidized state (Figure 8). At the maxima, the current increased by potential steps to increasing cathodic potentials, and shifted to shorter times when the initial state was obtained by oxidation at less anodic potentials (lower conformational packing degree). By integration the chronoamperograms, the chronocoulograms (see Supporting Information) are obtained. They represent reduction kinetics showing an induction period. The initial reduction rate can be obtained from the slope at the induction time (dQ/dt), the current at the original chronoamperometric maxima, through eq 6.

The kinetics of the n-doping reaction can be studied following a procedure similar to that presented for the p-doping reaction. By assuming a predominant interchange of cations during the process, the kinetic equation should be

$$r(\text{mol L}^{-1} \text{s}^{-1}) = \frac{dQ}{FV dt} = k[\text{TBA}^+]^\alpha [\text{Pol}^-]^\beta \quad (6)$$

Figure 10 shows the double logarithmic plot of the reduction rates versus different concentrations of active centers for n-doping; β reaction orders close to 2 were obtained. A good

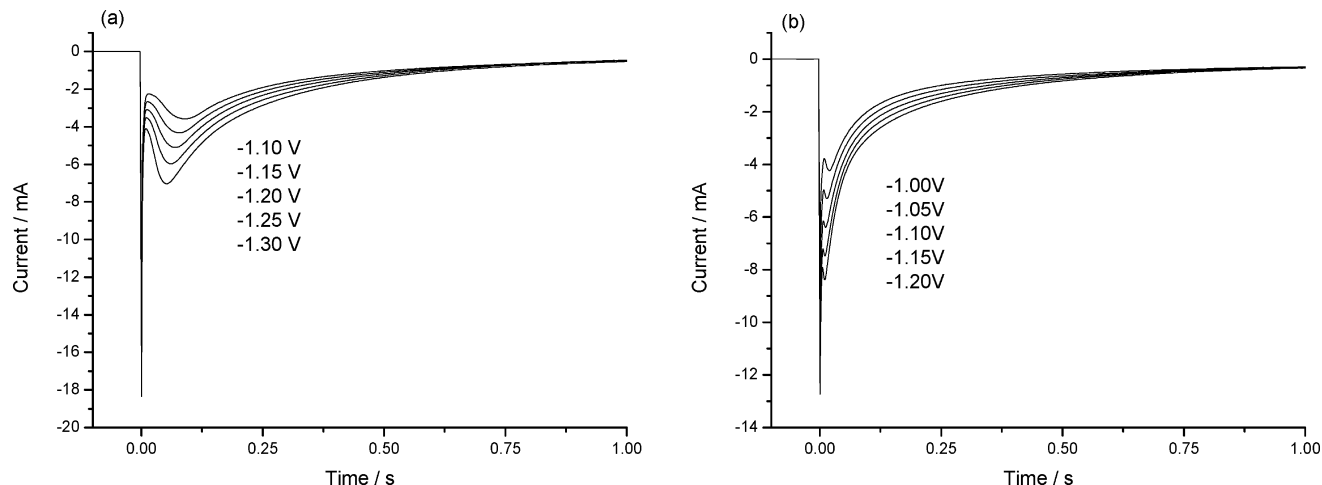


Figure 9. Chronoamperometric responses of a poly(2-ethylheptyl-DTCPD-co-3-methylthiophene)-coated platinum electrode in 0.1 M TBAPF₆ acetonitrile solution, submitted to potential steps from (a) 0.25 V and (b) 0.00 V anodic potentials maintained for 10 s to different cathodic potentials indicated in the figure.

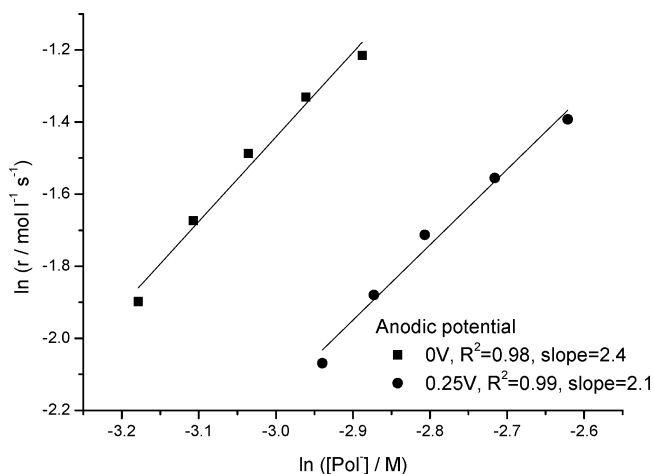


Figure 10. Double logarithmic plot of the oxidation rate of poly(2-ethylheptyl-DTCPD-co-3-methylthiophene) film submitted to potential steps between different indicated anodic potentials kept for 10 s every time and different cathodic potentials used in Figure 9 in 0.1 M TBAPF₆ acetonitrile solution.

fit of the experimental data is obtained, corroborating the chemical kinetic control of the n-doping process.

Conclusions

The modified-DTCPD monomer presents well-defined oxidation and reduction processes from solution but without generation of polymer films. A solution containing similar concentration of the modified-DTCPD monomer and 3-methylthiophene produces uniform films, quite stable under potential cycling. This material presents the characteristic redox processes of both the modified-DTCPD monomer and the poly-3-methylthiophene. A new process exists inside the n-doping region far away from the reduction of poly-3-methylthiophene, indicating a strong influence of a reduced comonomer neighbor, supporting the conclusion of copolymer formation during electropolymerization. By cycling between -0.25 and 1 V, a reverse electrochemical process is obtained, the mass of the film increasing by oxidation and decreasing by reduction. Storage of positive charges on the chains (p-doping) with entrance of PF₆[−] anions and solvent molecules from the solution and film swelling during oxidation is proposed.

At potentials more cathodic than -0.75 V, the film reduces, increasing its mass. Storage of negative charges on the chains

(n-doping) with entrance of balancing TBA⁺ cations and also solvent molecules from the solution and film swelling is proposed. A good fraction (up to 66%) of the negative charges, together with balancing cations, are not reoxidized at the beginning of the anodic potential sweep. They remain trapped and are oxidized concomitant with the storage of positive charges at high anodic potentials, resulting in a complex interchange of anions, cations, and solvent.

During p-doping, most of the trapped negative charges are compensated. By polarization between 0.2 and -0.75 V for long times, almost neutral states of the material are attained, with low densities of charge on chains and close packed conformational states. Using them as initial states to oxidize (p-doping) or reduce (n-doping) the material by potential steps, both processes give a maximum on the anodic (p-doping) or cathodic (n-doping) chronoamperometric responses. Initial rising currents indicate that the processes start under nucleation–conformational relaxation kinetic control. At the maximum, both processes occur under chemical kinetic control, allowing the determination of kinetic parameters.

Acknowledgment. We acknowledge financial support from Spanish Government (MCI) Projects MAT2008-06702 and CTQ2007-60459, Seneca Foundation Project 08684/PI/08, Consejería de Educación de Murcia, and Plan Regional de Ciencia y Tecnología 2007-2010. J.A.P. thanks the Ministerio de Ciencia e Innovación of Spain for Juan de la Cierva Grant JCI-2008-02022.

Supporting Information Available: Text giving full experimental details for the synthesis of 2-ethylheptyl-DTCPD copolymer, voltammetric characterization of poly (3-methylthiophene) film, chronocoulograms for p- and n-doping reactions, and evolution of the trapped charge per voltammetric cycle as a function of the cathodic potential limit. This information is available free of charge via the Internet at <http://pubs.acs.org>.

References and Notes

- (1) Rudge, A.; Raistrick, I.; Gottesfeld, S.; Ferraris, J. P. *Electrochim. Acta* **1994**, *39*, 273–287.
- (2) Conway, B. E. *J. Electrochem. Soc.* **1991**, *138*, 1539–1548.
- (3) Nishio, K.; Fujimoto, M.; Yoshinaga, N.; Furukawa, N.; Ando, O.; Ono, H.; Suzuki, T. *J. Power Sources* **1991**, *34*, 153–160.
- (4) Novak, P.; Muller, K.; Santhanam, K. S. V.; Haas, O. *Chem. Rev.* **1997**, *97*, 207–281.

- (5) *Organic Electronics: Materials, Manufacturing, and Applications*: Wiley-VCH Verlag: Weinheim, 2006.
- (6) Sirringhaus, H.; Tessler, N.; Friend, R. H. *Science* **1998**, *280*, 1741–1744.
- (7) Walker, W.; Veldman, B.; Chiechi, R.; Patil, S.; Bendikov, M.; Wudl, F. *Macromolecules* **2008**, *41*, 7278–7280.
- (8) Yang, C.; Cho, S.; Chiechi, R. C.; Walker, W.; Coates, N. E.; Moses, D.; Heeger, A. J.; Wudl, F. *J. Am. Chem. Soc.* **2008**, *130*, 16524–16526.
- (9) Skompska, M.; Mieczkowski, J.; Holze, R.; Heinze, E. *J. Electroanal. Chem.* **2005**, *577*, 9–17.
- (10) Ahonen, H. J.; Lukkari, J.; Kankare, J. *Macromolecules* **2000**, *33*, 6787–6793.
- (11) Arbizzani, C.; Catellani, M.; Mastragostino, M.; Mingazzini, C. *Electrochim. Acta* **1995**, *40*, 1871–1876.
- (12) Ding, H.; Pan, Z.; Pigani, L.; Seeber, R.; Zanardi, C. *Electrochim. Acta* **2001**, *46*, 2721–2732.
- (13) Montilla, F.; Pastor, I.; Mateo, C. R.; Morallon, E.; Mallavia, R. *J. Phys. Chem. B* **2006**, *110*, 5914–5919.
- (14) Ranger, M.; Leclerc, M. *Can. J. Chem.* **1998**, *76*, 1571–1577.
- (15) Otero, T. F.; de Otazo, J. M. G. *Synth. Met.* **2009**, *159*, 681–688.
- (16) Otero, T. F.; Arias-Pardilla, J.; Chermak, E. *Synth. Met.* **2009**, *160*, 425–431.
- (17) Otero, T. F.; Boyano, I. *J. Phys. Chem. B* **2003**, *107*, 6730–6738.
- (18) Otero, T. F.; Boyano, I. *J. Phys. Chem. B* **2003**, *107*, 4269–4276.
- (19) Otero, T. F.; Santos, F. *Electrochim. Acta* **2008**, *53*, 3166–3174.
- (20) Otero, T. F.; Abadías, R. *J. Electroanal. Chem.* **2008**, *618*, 39–44.
- (21) Otero, T. F.; Romero, M. C. *J. Phys. Conf. Ser.* **2008**, *127*, 012016.
- (22) Otero, T. F.; Grande, H.; Rodríguez, J. *J. Electroanal. Chem.* **1995**, *394*, 211–216.
- (23) Otero, T. F.; Grande, H. J.; Rodríguez, J. *J. Phys. Chem. B* **1997**, *101*, 3688–3697.
- (24) Otero, T. F.; Abadías, R. *J. Electroanal. Chem.* **2007**, *610*, 96–101.
- (25) Skompska, M.; Vorotyntsev, M. A.; Refczynska, M.; Goux, J.; Lesniewska, E.; Boni, G.; Moise, C. *Electrochim. Acta* **2006**, *51*, 2108–2119.
- (26) Arias-Pardilla, J.; Otero, T. F.; Blanco, R.; Segura, J. L. *Electrochim. Acta* **2010**, *55*, 1535–1542.
- (27) Vorotyntsev, M. A.; Casalta, M.; Pousson, E.; Roullier, L.; Boni, G.; Moise, C. *Electrochim. Acta* **2001**, *46*, 4017–4033.
- (28) Semenikhin, O. A.; Ovsyannikova, E. V.; Ehrenburg, M. R.; Alpatova, N. M.; Kazarinov, V. E. *J. Electroanal. Chem.* **2000**, *494*, 1–11.
- (29) Pigani, L.; Seeber, R.; Terzi, F.; Zanardi, C. *J. Electroanal. Chem.* **2004**, *570*, 235–242.
- (30) González, H. Master Thesis, Universidad Politécnica de Cataluña, 2004.

JP1038865